INNOVATION IN WOODWORKING INDUSTRY AND ENGINEERING DESIGN, 1/2014 (5): 103–110

JOINT RESEARCH INTO DYNAMICS AND STRENGTH OF BANDSAW BLADES IN ROSENHEIM FACULTY OF WOOD TECHNOLOGY, GERMANY

Stefan Stefanov[1], Frieder Scholz[2]
[1]University of Forestry, 10 Kliment Ohridski blvd, 1797 Sofia, Bulgaria,
e-mail: stefanov_sh@abv.bg
[2]University of Applied Sciences, Rosenheim, Germany, e-mail: scholz@fh-rosenheim.de
[1]borislav65@abv.bg, [2]ralitsa_t_s@abv.bg

ABSTRACT

During DAAD 2013 research stay of the first author in Rosenheim Faculty of Wood Technology, joint research started into dynamics and strength of bandsaw blades. This paper is, in fact, the first one under the above title resulting from cooperation with Professor Scholz and his team. They have dealt with problems concerning dynamic instability of new sawblades with special crowned tooth shape. Studies had been carried out under various blade-tensioning and guide-system conditions. Now, FE analysis has been involved by means of Autodesk Inventor software. An approach has been proposed and developed for FE modelling the complicated buckling of bandsaw blades by substituting it with a sufficiently equivalent eccentric compression. Research results and conclusions on the reasons for the instability of blades with crowned tooth shape are presented.

Key words: bandsaw blade, instability, crowned tooth shape, FE analysis

INTRODUCTION

According to (Scholz *et al*. 2013), cemented carbide teeth and stellite teeth have been used for years as a means of improving cut quality and wear-resistance on circular saw blades. Only recently such teeth have been used on bandsaw blades to achieve equivalent results. The ideal tooth design would produce a surface which requires little or no post-cut processing. In response to Industry demand, FH has partnered in a joint project with Alber Saw Blades, KaehnyGmbh, and the Institute for Machine Tools at the University of Stuttgart. The objectives have been: increasing the time between sharpening, increasing fatigue strength, solidifying the gullet, enlarging solder area, and reducing the effect of vibrations and washboarding. As well, testing a new magnetic guide system (Flying Bandsaw of Esterer WD Gmbh) has been set.

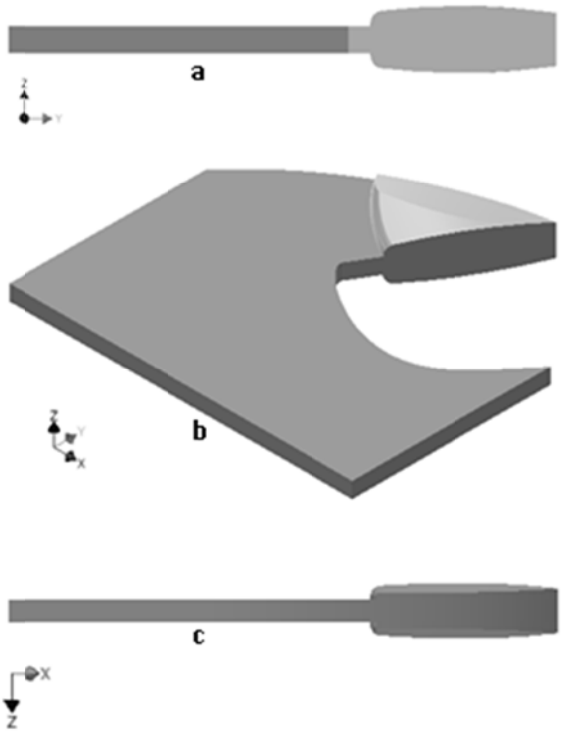

Figure 1: The crowned tooth shape
a – tooth face view; b – isometric view;
c – tooth back view

Figure 2: The failure of the saw blade

In the project mentioned, a crowned (oval) tooth face shape has been applied. It is shown in Fig. 1 (an Inventor model). This special shape was successful at router blades, circular saws, and was used in the production of high-precision airplane windows. Therefore, decision was made to test this shape on a bandsaw. And, during the first test, the saw blade veered off the cutting line and cut deeper into the log until failure occurred (Fig. 2). Neither the traditional guide blocks nor the state-of-the-art magnetic guide system were able to stabilize the sawblade.

The authors of (Scholz *et all*. 2013) have done analysis of the lateral forces at the crowned cutting edges. Thus, they explain to a certain extent what the reasons for the blade failure are. However, as they say, this seems not to be the sole answer for the observed instable behavior. The central thrust force exerting compression on the main cutting edge may cause buckling of the sawblade. The authors state that further more sophisticated theoretical approaches are needed to completely identify the reasons for the instable blade behavior.

1. THEORETICAL FINITE-ELEMENT STUDY ON TWIST-BEND BUCKLING OF A BLADE

In Fig. 3, a beam is shown as a model corresponding to a bandsaw blade where $b >> s$. The illustration is a 3D Inventor assembly model with overlapped additional graphics (as done also in next figures). The force P is uniformly distributed with an intensity $q = P/l$. The two slot supports of the beam can pivot on two grounded pins having Inventor Fixed Constraints (such constraints are illustrated by crosshatching).

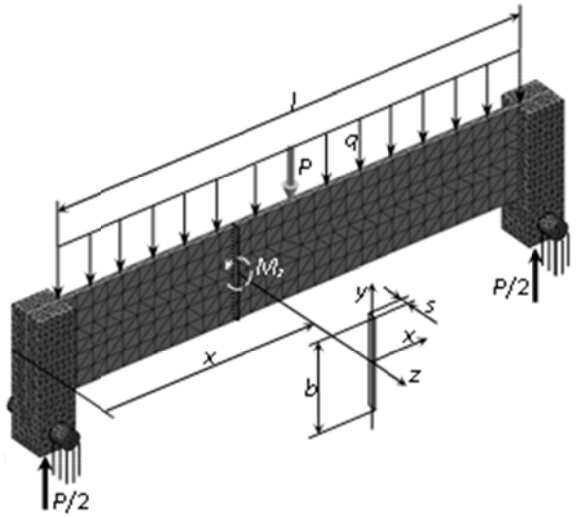

Figure 3: A beam as a model of a blade

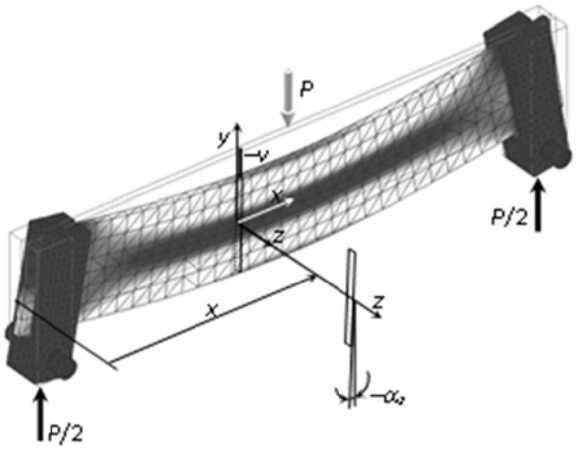

Figure 4: Bending in the plane *x-y*

The beam is much stiffer against bending in the plane x-y where the bending moment M_z acts, and is very flexible in the perpendicular plane x-z (if a bending moment M_y acts there). In Fig. 3, the beam is loaded in the stiff plane x-y with $M_z(x) = xP/2 - q_y x^2/2$, whereas $M_y = 0$. The bending appears as shown (exaggeratedly) in Fig. 4. Deformational displacement $v = v(x)$ of the cross section center in the y direction is available.

Meanwhile it is to clarify that in this paper displacements of (centers of) cross-sections in the directions x, y, z are denoted as u, v, w (Stefanov 2007); concretely in Fig. 4, $u = 0$, $w = 0$, and $v = v(x) \neq 0$ is negative. As to the angles of deformational tilts (rotations) of cross-sections around the beam's axes x, y and z, they are denoted as $\varphi \equiv \alpha_x$, $\alpha \equiv \alpha_y$ and α_z (Stefanov 2007); in Fig. 4, $\varphi = 0$, $\alpha_y = 0$, and $\alpha_z = \alpha_z(x) \neq 0$ is negative.

It is well known that at a sufficiently high, critical magnitude P_{cr} of P, the beam will buckle out sidewise (Fig. 5) due to $b >> s$. This buckling is a twist associated always with second bending in the perpendicular plane x-z of flexibility.

The main characteristic of buckling is that it is possible since sufficiently great forces can take displacements as moment arms. In the usual case of deformation, moment arms of forces are always associated with initial dimensions of the body. If there are no initial arms, there will be no initial moments: no torsional and bending moments M_x and M_y in Fig. 3. However, displacements can come first and serve as moment arms. Thus, let a displacement $-w(x)$ come first in Fig. 5 as an arm of q for $M_x(x)$. Then, torsion with the angle φ occurs and the final arm of q for $M_x(x)$ is $\delta_z(x) = -w(x) - b\varphi/2$. Next, the expression of $M_x(x)$ should be obtained. This is not simple since P is not concentrated but distributed along the top face of the beam. Next, since the principal axes y and z of inertia of the cross section have been tilted by φ to the new positions labeled as (y) and (z), q should be resolved into $q_{(y)}$ and $q_{(z)}$. This is a situation for double bending: appearance of $M_y(x)$ due to $q_{(z)}$ together with $M_z(x)$ due to $q_{(y)}$.

Next, two differential equations of second order for $w(x)$ and $\varphi(x)$, bound together, should be worked out and solved. The boundary conditions at the ends of the beam are $\varphi = 0$ and $\alpha_y = w'(x) = 0$ provided by reactive moments $M_{R,x}$ and $M_{R,y}$ (Fig. 5). The problem of setting the two differential equations and their solution for finding out P_{cr} is not easy at all. The reader can look at and follow how similar easier problems are set and solved in Advanced Strength of Materials courses, e.g. in (Den Hartog 1984).

Besides, for better approaching of the model in Fig. 5 to a real bandsaw blade, the following modifications should be done. An internal longitudinal force $N_x(x)$ of tensioning the blade should be added to Fig. 5, with $-w$ moment arm, which tries for straightening the beam, respectively for preventing it from buckling and stabilizing it; P_{cr} should increase then. The length of the beam should be stretched far off the two supports to reach the bandsaw wheels. The two guide-system supports of a real blade do not look like the slot supports in Fig. 5 and would not provide the conditions $\varphi = w = 0$ and $\alpha_y = 0$ exactly; etc. Hence, an exact mathematical solution for P_{cr} of a real bandsaw blade becomes totally impossible, practically.

Nowadays, the existing FE systems have radically changed the approaches to

problems of deformation and strength. Any deformable body of arbitrary geometry can be arbitrarily loaded and constrained. Any stress, strain and displacement of any finite element can be obtained. This generates ideas and solutions that are not implementable by means of the classical courses of Strength of Materials and Theory of Elasticity. FE software can also indirectly help in cases where it cannot provide direct solutions. Such cases relate to differential equations of buckling (unfortunately), forced vibrations, etc., which cannot be set for arbitrary geometry, loading and constraints.

Thus, Fig. 5 does not directly represent a real buckling. The illustration has been obtained, in fact, by applying the force P eccentrically: not to the center of the beam's top face like in Fig. 3, but to the rear edge of that face, i.e. with eccentricity $s/2$. Respectively, in the original Inventor display of Fig. 5, P does not move at the distance $\max\delta_z$ but stays at its initial position in the middle of the edge (similarly, in Fig. 4, P stays in its initial position).

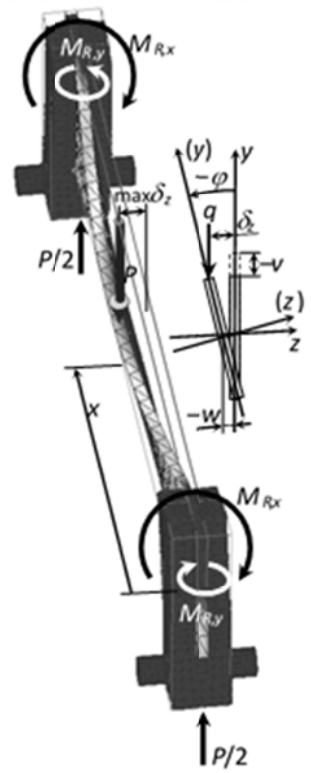

Figure 5: Buckling

In fact, the buckling has been approximated by eccentric compression. This is an essential feature of this paper: advancing an idea for determination of P_{cr} (respectively, $q_{cr} = P_{cr}/l$) after substituting the buckling with eccentric compression. Of course, a condition should be formulated to provide sufficient equivalence between the buckling and the eccentric compression. For Fig. 5, the condition in question states: P becomes P_{cr} when $\max\delta_z$ (shown exaggeratedly) equalizes the eccentricity (which is $s/2$ in the case considered). Indeed, then P has the same moment arm to the initial x-z plane both in case it is initially centrically located but later displaced at $\max\delta_z$ by the deformation, and in case it is not displaced later but is initially eccentrically located at $s/2 = \max\delta_z$. For better grounding such a condition and estimating insofar it provides $P = P_{cr}$, a corresponding analysis of the well-known first Euler case of buckling of a compressed

column follows under the additional subheading 1.1 below.

Thus, the way is opened for a method of approximation of the saw blade buckling, which is otherwise impossible to be found out theoretically, by FE eccentric compression simulation. According to 1.1, the error in P_{cr} determination is expected to be about 20 per cent on the safety side. As an example, a saw blade buckling approximation model is shown in Fig. 6 where s = 1 mm, b = 84 mm (to the gullet bottom), l = 816 mm. Six forces have been applied with an eccentricity of $s/2$ = 0,5 mm providing $s/2 \approx \max\delta_z$. They total $P = P_{cr}$ = 6 kN.

This P_{cr} magnitude of P is too high due to $\varphi = w = \alpha_y = 0$ provided by the slot supports, and provided that the blade would bear stresses about 1000 MPa. Additional reasoning and computing can be done for actual guide supports after estimating the non-zero φ, w and α_y they would allow. Besides, two opposite forces should be applied at the two ends of the blade for tensioning and stabilizing it, as discussed above. The line of action of the two forces should have an eccentricity which equalizes the corresponding displacement δ_z as a moment arm. Then P_{cr} will have to be greater to enable $s/2 \approx \max\delta_z$.

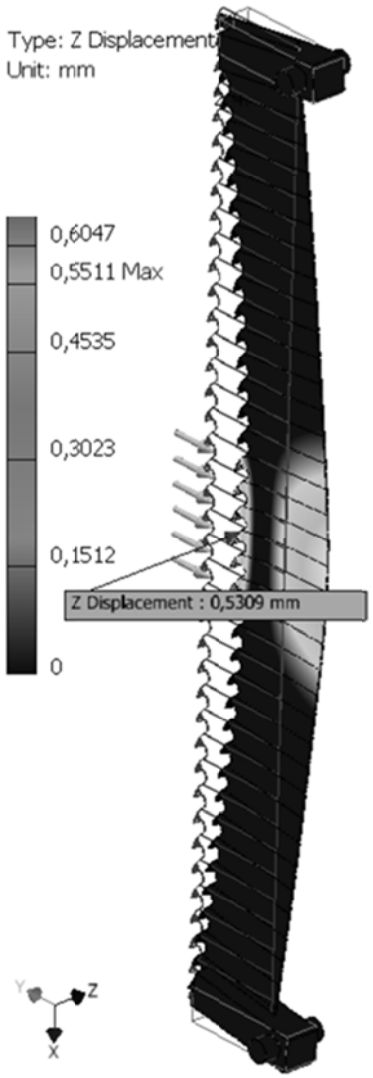

Figure 6: Saw blade buckling model

1.1. BUCKLING OF A COMPRESSED COLUMN APPROXIMATED BY ECCENTRIC COMPRESSION

Fig. 7 represents the first Euler case (imagine P is centrically located). The column has dimensions 10x10x200 mm. To apply the Euler equation $P_{cr} = \pi^2 EJ/(2l)^2$ (Stefanov 2007), in the case in hand we have l = 0,2 m and $J = 10^4/12$ = 833,3 mm^4 = 833,3.10^{-12} m^4. Suppose steel with E = 2,05.10^{11} Pa. Hence, P_{cr} = 10 538 N.

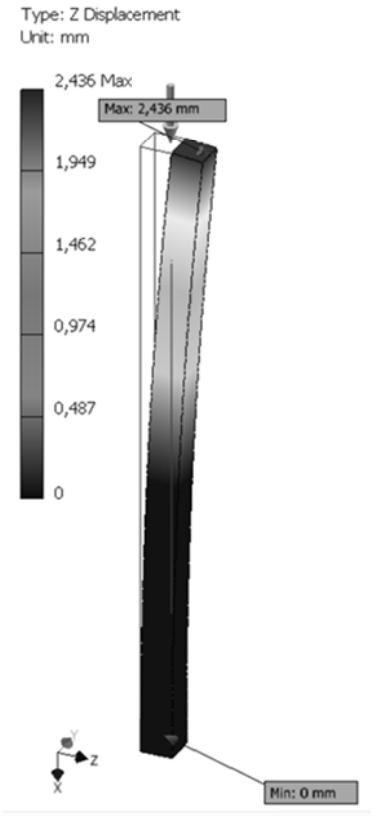

Figure 7: First Euler case approximated

Now let the force P have an eccentricity e. According to Strength of Materials courses, e.g. (Stefanov 2007), it is easy to work out that $Pel^2 = 2EJ.\max\delta_z$. Upon equalizing $e = \max\delta_z$ and canceling it out, the equation $Pl^2 = 2EJ$ remains, i.e. $P = 8EJ/(2l)^2$. By comparing with $P_{cr} = \pi^2EJ/(2l)^2$ it proves that $\pi^2 = 9{,}87$ is replaced by 8.

Hence, if substituting the buckling with eccentric compression, regardless of what $e = \max\delta_z$ is (it cancels out), we can accept $P = 8EJ/(2l)^2$ as approximating P_{cr} by an error factor of $8/\pi^2 = 0{,}8106$. In the case of Fig. 7, the lower, approximated P_{cr} is 0,8106.10538 = 8542 N. This magnitude of P has been applied to the FE model in Fig. 7 and the following result appeared, indeed: $\max\delta_z = 2{,}436 \approx 2{,}5$ mm where 2,5 mm = e is the eccentricity set. If resetting e with a different value, the approximated force $P_{cr} =$ 8542 N produces again $\max\delta_z \approx e$.

The reason for the approximated P_{cr} to be lower than the Euler P_{cr} is due to replacing the Euler sinusoidal deflection line with the eccentric compression deflection line. Only one displacement $\max w \equiv \max\delta_z = e$ as a moment arm of P agrees with the Euler deflection. The rest of the eccentric compression deflection displacements $w(x)$ are a bit greater than the Euler $w(x)$. Anyway, the condition $\max\delta_z = e$ provides acceptable approximate equivalence between eccentric compression displacement $w(x)$ and the actual buckling displacement $w(x)$.

2. FINITE-ELEMENT COMPARATIVE STUDY ON LATERAL PRESSURES ON CROWNED AND STANDARD TEETH

When the saw blade is located in the slot cut, P_{cr} in the case of Fig. 6 will increase many times as much. Some FE modeling results (not placed in this paper) confirm this. Besides, by comparison, from the first Euler case to the fourth one, P_{cr} increases 16 times: $P_{cr} = \pi^2EJ/(2l)^2$ becomes $P_{cr} = \pi^2EJ/(0{,}5l)^2$ (Stefanov 2007). Thus, it is to expect that inevitable loading eccentricity causes the problems with the crowned teeth rather than buckling. That is why, the FE study has been directed to comparison of lateral (in z direction) pressures on crowned and standard cutting edges.

Several different FE models have been created and examined. They have simulated the interaction of a blade (like that one in Fig. 6), a wood-piece with a slot cut in which the blade is located and pushed, and a holder of the wood-piece. It is not easy to provide the agreement of the FE model with the actual interaction of the teeth, the wood-piece and the other assembly components. Even if full adequacy is not achieved with a

given model and the results from it could not be considered as absolute, the model provides, anyway, a basis of comparative study and comparative results.

In this paper, the last of the created models is shown (Fig. 8). Its dimensions, shapes, numerical data, constraints etc. do not claim for absolute adequacy but serve for the purposes of the comparative analysis. Like in Fig. 6, s = 1 mm, b = 84 mm, l = 816 mm. The kerf is 2,5 mm. The wood-piece is of cherry. The holder is of steel and would pivot on its fixed (crosshatched) edge. It is additionally supported by a reactive force R of a spring having k = 122,2 N/mm. The pushing force P is 200 N and is applied at the level of the holder's fixed edge. This means eccentric application of P towards the blade. Such a situation of eccentric pushing and holding by lateral force R is not far from real operational conditions: exact centricity for P could not be provided.

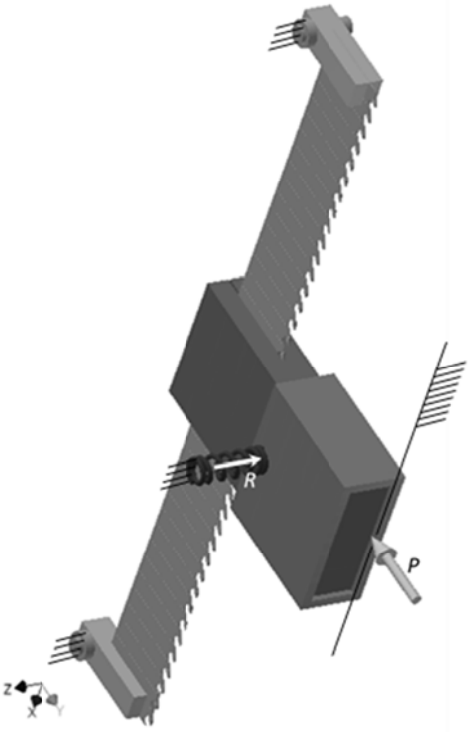

Figure 8: The model in consideration

Fig. 9 illustrates a standard-shaped tooth and is analogous to Fig. 1. The dimensions are the same, including the kerf, but the lateral edges of the tooth's face are now standard, i.e. not crowned but straight. Both in Fig. 1 and Fig. 9 the main cutting edge is idealized to have no fillet. Then, unreal high local stresses may appear. They will not deteriorate but emphasize the comparisons.

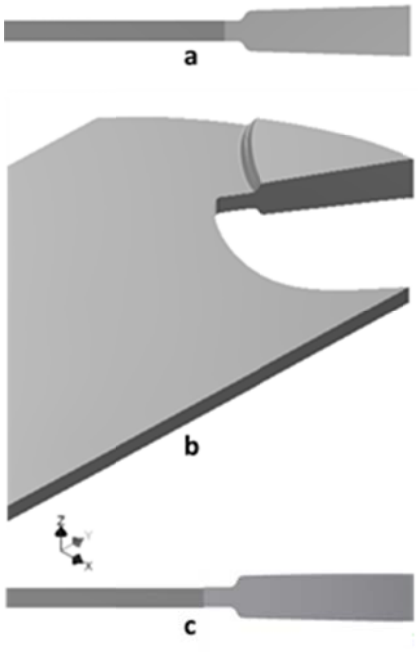

Figure 9: Standard-shaped tooth

Fig. 10 shows the (exaggerated) deformation and Von Mises Stress of the assembly with standard teeth. After disabling Visibility of the other components, the Max Von Mises Stress of 194,3 MPa is revealed as shown in the fragment to Fig. 10.

Fig. 11 shows Max Contact Pressure Z (lateral) of 6,336 MPa. It remarkably does not appear at the lateral cutting edge of the tooth's head but at the lateral edge of the tooth's back: the mutual deformation with the internal surface of the slot is such that the tooth's head is free from lateral pressure.

Next, the standard teeth in the slot cut have been replaced with crowned teeth.

Their behaviour is quite different now, as follows.

The Max Von Mises Stress is 6018 MPa and appears at the crowned lateral cutting edge, Fig. 12a (compare with Fig. 10 where the counterpart stress is on the main cutting edge, and is 194,3).

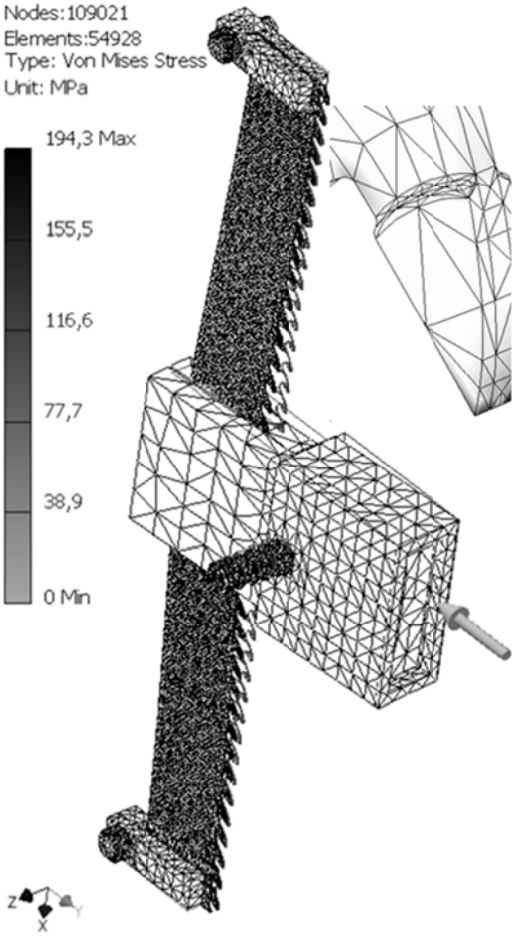

Figure 10: Standard teeth FE model

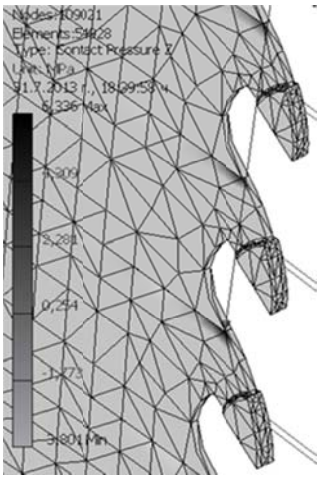

Figure 11: Standard teeth Max Contact Pressure Z

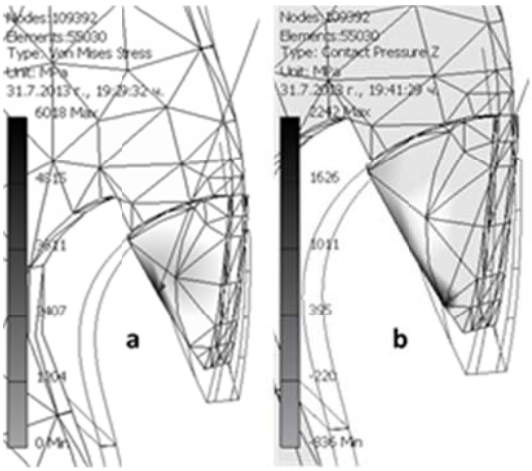

Figure 12: Crowned tooth behaviour

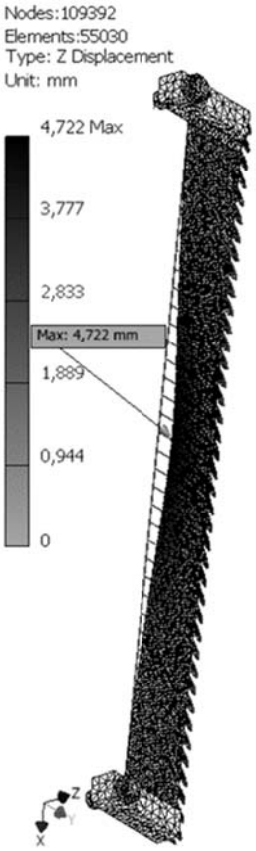

Figure 13: Ready to veer

The Max Contact Pressure Z (lateral) is 2242 MPa and again acts on the crowned lateral cutting edge, Fig. 12b (compare with Fig. 11). The Max Z (lateral) Displacement of the blade is 4,722 mm, Fig. 13 (compare with standard teeth: it proves 0,4438 mm there). On the other hand, the Z displacement at the moving spring end (not

illustrated) has proved nearly twice as short as in the case of standard teeth (*R* is about 15 N now). The tooth oval is obviously a spot of pivoting.

Hence, the blade with the crowned teeth is ready to veer (Fig. 13) once cutting starts and the slot cut is still short. Whereas, according to the previous illustrations and data, the blade with the standard teeth will remain and behave quietly in a long slot cut.

Additional results (not placed in this paper) have also been obtained after decreasing *P* twice as little, i.e. to 100 N. Then the behaviors of the crowned and standard teeth trend to equalizing.

CONCLUSION

The FE modeling done certainly throws additional, sophisticated light revealing why the blade with crowned teeth is instable. After this first step of cooperation with FH, in next studies more elaborated FE models would be developed. Incisions and chips cut would be formed in front of each tooth, more actual constraints and contacts at the guide system and the wheels would be set, the longitudinal forces for blade tensioning and cutting would be included, and so on. FE revealing the concentrated local stresses immediately helps for designing and redesigning of solidified gullets, enlarged solder areas, etc.

REFERENCES

1. Den Hartog J. P. (1984). Advanced Strength of Materials. Dover Publications, Mineola, NY
2. Scholz F., Großmann M., Tröger J., Heisel U., Hemer A., Keller T., Foertner R., Ratnasingam J. (2013). Performance of Crowned Edges on Band Saws. 21st International Wood Machining Seminar Proceedings, Tsukuba, Japan, IUFRO Publishing: 222–229
3. Stefanov S. (2007). Strength of Materials. Publishing house of UF, Sofia (in Bulgarian)